



POTSDAM-INSTITUT FÜR  
KLIMAFOLGENFORSCHUNG

**Originally published as:**

Raj, S., [Shukla, R.](#), Trigo, R. M., Merz, B., Rathinasamy, M., Ramos, A. M., Agarwal, A. (2021): Ranking and characterization of precipitation extremes for the past 113 years for Indian western Himalayas. - International Journal of Climatology, 41, 15, 6602-6615.

DOI: <https://doi.org/10.1002/joc.7215>

1 **Ranking and Characterization of Precipitation Extremes for the past 113 years for Indian**  
2 **western Himalayas**

3

4 Saurav Raj<sup>1</sup>, Roopam Shukla<sup>2</sup>, Ricardo M. Trigo<sup>3</sup>, Bruno Merz<sup>4</sup>, Maheswaran Rathinasamy<sup>5</sup>,  
5 Alexandre M. Ramos<sup>3</sup>, Ankit Agarwal<sup>4,6,\*</sup>

6

7 <sup>1</sup>Department of Civil Engineering, Indian Institute of Technology Roorkee, 247667  
8 Uttarakhand, India

9 <sup>2</sup>Potsdam Institute for Climate Impact Research (PIK), Member of the Leibniz Association,  
10 Telegrafenberg, 14473 Potsdam, Germany

11 <sup>3</sup>Instituto Dom Luiz, Faculdade de Ciências, Universidade de Lisboa, 1749016 Lisboa, Portugal

12 <sup>4</sup>GFZ German Research Centre for Geosciences, Section 4.4: Hydrology, Telegrafenberg,  
13 Potsdam, 14473 Germany

14 <sup>5</sup>Department of Civil Engineering, MVGR College of Engineering, Vizianagaram, 535005 India

15 <sup>6</sup>Department of Hydrology, Indian Institute of Technology Roorkee, 247667 Uttarakhand, India

16

17

18 **\*Correspondence to: Ankit Agarwal (ankit.agarwal@hy.iitr.ac.in)**

19

20

21

22

23

24

25

26

27

28

29

30

31

32

33

34

35  
36  
37  
38  
39  
40  
41  
42  
43  
44  
45  
46  
47  
48  
49  
50  
51  
52  
53  
54  
55  
56  
57  
58  
59  
60  
61  
62  
63  
64  
65  
66

## Abstract

Globally, mountain systems are unevenly exposed to risks of extreme precipitation. Within the Himalayan region, precipitation extremes are a rising concern, but their current understanding is limited. In this study, we use 113 years of precipitation data to rank and characterise precipitation extremes in the Indian Western Himalayas (IWH). Our statistical ranking method integrates precipitation spatial extent and its intensity across different durations for determining the severity of extreme events. The proposed ranking method advances conventional single-day event ranking methods by accounting for multi-day duration to capture persistent precipitation episodes. Results show that the method accurately detects and ranks the most extreme precipitation events that occurred in the IWH and indicate locations of these events. Our results highlight that critical long duration events in the region (e.g. 10 days) are missed at ranks at shorter duration (e.g. 2-3 days), thereby highlighting the importance to multi-day precipitation extremes ranking. In addition, the proposed ranking method provides information with confidence about the event duration that will be associated with the highest impact on society, carrying high significance. Our findings are valuable for flood risk management and disaster risk reduction.

**Keywords:** Precipitation; Extreme; Multi-day ranking; Western Himalayas; Climate Change, Mountains

## 67 1 Introduction

68 Human-induced global warming is changing the frequency and magnitude of weather-related  
69 extremes (Pachauri et al., 2014). In particular, intense precipitation events and associated risks  
70 are expected to occur more frequently over Asian regions, especially over India, Bangladesh,  
71 and China (Goswami et al., 2006; Parry et al., 2007). Although a uniform and consistent decrease  
72 in moderate precipitation has been reported across India (Ghosh et al., 2012), precipitation  
73 extremes have changed in a heterogeneous way over India in the past half-century (Rajeevan  
74 et al., 2006; Krishnamurti et al., 2013; Guntu et al., 2020). This variability in the occurrences of  
75 precipitation extremes in space and time is a consequence of different interacting drivers and  
76 complex geographical features (Nicholls et al., 2012).

77 The Indian Western Himalayan (IWH) region is prone to severe weather conditions due to the  
78 joint mechanism of the Indian Summer Monsoon (ISM) and Western Disturbances (WDs). ISM  
79 is usually relevant between June and September (JJAS), and WD is dominant from December to  
80 March (DJFM, Krishnan *et al.*, 2019). The climate of the Himalayas is strongly influenced by  
81 different types of wind systems, such as mesoscale cyclonic storms, snowstorms, and other  
82 high-speed winds along with cloudbursts (Das and Meher, 2019). The combination of these  
83 highly energetic phenomena and the pronounced orography often results in sudden  
84 precipitation extremes (Nandargi and Dhar, 2011) that cannot be predicted effectively. While  
85 daily and sub-daily precipitation extremes usually result in urban and small stream flash  
86 flooding, long-duration precipitation episodes can lead to large-scale river floods, inducing  
87 major socio-economic impacts (Shukla et al., 2019; Kumari et al., 2019) and other adverse  
88 consequences such as deep landslide movements (Ozturk et al., 2018). Precipitation extremes  
89 have become a severe concern in recent decades in the IWH region due to higher vulnerability  
90 of the society to such events (Das and Meher, 2019).

91 Several studies have attempted to understand the past changes of extreme precipitation events  
92 in the IWH; however, two major gaps remain. Firstly, past assessments are restricted to limited  
93 spatial extents often based on a case-by-case approach for a few stations only (Nandargi et al.,  
94 2016, Kumari et al., 2019, Priya et al., 2017). Secondly, ranking and characterisation of extreme  
95 precipitation events using high-resolution long-term data at high spatial scale are scarce over  
96 India, and absent for the IWH region, to the best of our knowledge. To fill these gaps, we analyze  
97 the spatio-temporal changes in the precipitation extremes using a high-resolution and long-  
98 term dataset. This understanding will be extremely useful to inform disaster management and  
99 to develop risk reduction strategies to mitigate adverse impacts. For instance, a simultaneous

100 increase in magnitude and spatial extent, as shown for river floods in some regions of Europe  
101 (Kemter et al., 2020), represents important information for emergency response and disaster  
102 recovery. In fact, as the probability of simultaneous events increases it implies that resources  
103 and funds need to be provided at many locations at the same time.

104 Several methods have been proposed in recent years to rank and characterise extremes in  
105 different regions of the world. For instance, Müller and Kaspar (2014) developed an 'event-  
106 adjusted' method based on the optimization of the event area and the time duration. Ren et al.  
107 (2012) presented a similar threshold-based objective method for identification of regional  
108 extreme events considering their impact area and duration. Ramos et al. (2014, 2017)  
109 developed an objective ranking method to evaluate daily precipitation and multi-day  
110 precipitation extremes by taking into account both the area and average intensity of the event.  
111 They used a season-dependent definition for extreme events emphasising that these must have  
112 large departures from climatology. Beguería et al. (2009) presented a methodology for  
113 continuous seasonal mapping of peak intensity, magnitude and duration of extreme  
114 precipitation events based on the extreme value theory for a region in the north-eastern Iberian  
115 Peninsula. With the aim of quantifying the severity of large-scale flood events, Uhlemann et al.  
116 (2010) and Schröter et al. (2015) defined a severity index, which considers both spatial extent  
117 and magnitude by integrating the flood-affected river network length with the flood magnitude.

118 Our study has two main objectives: (i) to understand the seasonal and long-term changes in  
119 frequency and magnitude of extreme events over the 113-year period 1901-2013 for IWH; and  
120 (ii)-to develop an objective ranking of extreme precipitation episodes for different durations  
121 (from 1 to 10 days) for the entire IWH exploiting the long-term, high-resolution precipitation  
122 dataset. The study provides important information on the seasonality and long-term trends in  
123 the frequency of extreme precipitation events, along with information on the locations of the  
124 highest ranked events. Further, the study objectively ranks and characterises the nature of  
125 extreme precipitation events for the 113-year period using a statistical approach adapted from  
126 Ramos et al. (2014, 2017). It incorporates three matrices, i.e. spatial extent, magnitude, and  
127 duration, for ranking the extreme event. The rationale behind this approach is to integrate,  
128 besides the event intensity, its spatial extent and duration, as these characteristics can be  
129 decisive for the event impact on society (e.g. Uhlemann et al., 2010, Dung et al., 2015). Hence,  
130 the highest-ranked events have a large spatial spread and, simultaneously, are characterised by  
131 large departures from the local climatology for that time of the year. After combining the

132 information on magnitude and spatial extent, we examine and include the information on the  
133 duration of each event.

## 134 2 Study Area

135 The Himalayan mountain range plays a dominant role in controlling the weather and climate of  
136 the Indian subcontinent (Krishnan et al., 2019). As demonstrated by Krishnan et al. (2019)  
137 through numerical model simulations, the 'southwest monsoon' will cease to exist if the  
138 'Himalayas' are removed from their current position. The rugged topography enhances heavy  
139 rainfall in the river catchments of the Himalayas resulting in hydrometeorological extremes  
140 with cascading adverse impacts on humans, their assets and the environment (Pandit, 2013,  
141 Priya et al., 2017). Monsoonal rainfall (JJAS) and Western Disturbances (DJF) are two major  
142 atmospheric circulation patterns bringing rainfall in IWH, consisting of the three states Jammu  
143 & Kashmir (JK), Himachal Pradesh (HP) and Uttarakhand (UK) (Fig. 1a).

144

145 *[Please insert figure here]*

146 **Figure 1: (a) Topography of the Indian Western Himalayas (IWH) consisting of the three**  
147 **states Jammu & Kashmir (JK), Himachal Pradesh (HP) and Uttarakhand (UK), (b) annual**  
148 **frequency and (c) seasonal frequency of occurrence of precipitation-related disasters in**  
149 **the IWH region since 1900 as per EM-DAT data (D. Guha-Sapir et al n.d.,) (d) annual**  
150 **number of deaths in the IWH region due to hydro-climatological hazards as per EM-DAT**  
151 **data.**

152 The IWH region showcases a complex topography with elevation ranging from 184 m in the  
153 valleys to 8500 m at mountain peaks (Fig. 1a). The complex topography strongly affects the  
154 spatial distribution of rainfall (Joshi and Kumar, 2007; Kumari et al., 2017). Increasingly,  
155 extreme weather conditions and natural disasters are becoming common in IWH (Fig. 1b), and  
156 in most cases, disasters are triggered by high rainfall events. There is a strong seasonal pattern  
157 in the frequency of events (Fig. 1c) with disasters occurring mainly during monsoonal rains and  
158 WDs. The frequency of disaster occurrence in the IWH region increased significantly in the 20th  
159 century. Moreover, trends in annual losses in terms of the number of deaths shows a  
160 remarkable increase after 1990 (Fig. 1d). The extremes and related disasters over these years  
161 caused high socioeconomic impacts in terms of casualties, affected people, and economic losses.  
162 The observed trend of precipitation extremes has direct implication not only for the

163 communities in the IWH, but also for water-resource managers and decision makers, as  
164 growing risks demand preparedness decisions (Singh et al., 2014).

### 165 3 Data and Method

#### 166 3.1. Precipitation data

167 We use the high-resolution (0.25°×0.25°) gridded daily rainfall data from the Indian  
168 Meteorological Department (IMD) developed by Pai et al. (2014). Given the sparse and uneven  
169 distribution of rain gauges in the region, a gap-free, continuous and gridded data was generated  
170 using daily rainfall measurements. The station data was converted to gridded data through  
171 spatial interpolation by employing the Inverse Distance Weighted scheme. The data is freely  
172 available at the archive of the National Data Centre, IMD, Pune (see section data sources) for  
173 the period 1901 to 2013.

174

#### 175 3.2. Ranking method

176 It can be rather difficult to evaluate extreme events that cover areas with significant differences  
177 in the average precipitation on a daily scale. This difficulty is further compounded by large  
178 differences in the variability of the local precipitation. Therefore, the use of daily normalized  
179 precipitation anomalies (that take into account the different variability range in each grid  
180 point) corresponds to a key step to obtain a meaningful ranking of daily precipitation extremes  
181 in the IWH (Ramos et al., 2014). It allows characterizing each day taking into account not only  
182 the severity of the precipitation but also the associated spatial extension. To rank precipitation  
183 extremes over multi-day accumulated periods, a three-step method is used, following the  
184 methodology previously developed Ramos et al. (2017).

185 **Step 1:** We use the daily normalized precipitation anomalies ( $A_{c,i,j}$ ) given by

$$A_{c,i,j} = \frac{P_{c,i,j} - \mu_{c,i,j}}{\sigma_{c,i,j}} \quad (1)$$

186 where  $P_{c,i,j}$  is the precipitation value,  $\mu_{c,i,j}$  is the daily Julian mean, and  $\sigma_{c,i,j}$  is the daily standard  
187 deviation (SD) for a particular year and day ( $c$ ) and for a particular grid point ( $i, j$ ). Only days  
188 with precipitation above 1 mm (wet days) are taken into account in the computation of the daily  
189 climatological series. The daily Julian mean and SD are computed for the entire observational  
190 period 1901-2013 (i.e. 113 years). A 7-day running mean is applied afterwards to the

191 climatological series to smooth the noisy time series. Therefore, for each day and each grid  
 192 point, a normalised precipitation departure from climatology is computed.

193 **Step 2:** We compute the accumulated precipitation anomalies (Eq. 2) for a certain period  $p$  over  
 194 multi-day periods ( $n$ ).

$$AA_{C,i,j} = \sum_{c=1}^n A_{C,i,j} \quad (2)$$

195 The 3-day accumulated precipitation anomaly, for example, on 5 September 1995 corresponds  
 196 to the sum of the normalized precipitation anomalies relative to 3-5 September 1995.

197 **Step 3:** The final step computes the magnitude of the precipitation extreme for each  
 198 accumulated precipitation anomaly period. We have adopted the procedure proposed by  
 199 Ramos et al. (2014). The magnitude of extreme events is given on a daily basis by an index that  
 200 is obtained after multiplying two values:

- 201 ● the area (**A**, in percentage of IWH) that has precipitation anomalies (at each time scale)  
 202 above 2 standard deviations SD, and
- 203 ● the mean value of these anomalies (**M**) for all the grid points that are characterized by  
 204 precipitation anomalies above 2SD.

205 So, for single-day ranking, the magnitude (**R<sub>d</sub>**) is calculated using a single-day anomaly ( $A_{c,i,j}$ )  
 206 and for multi-day rankings, the magnitude (**R<sub>m</sub>**) is computed using the accumulated anomaly  
 207 ( $AA_{c,i,j}$ ) for that day over all grid points. The 2SD threshold corresponds roughly to the 95%  
 208 percentile of the daily precipitation distribution at each grid point. However, the methodology  
 209 can be easily adapted, for instance, by increasing the SD threshold when particularly extreme  
 210 events are of interest.

### 211 3.3 Selection of critical duration of extreme event ranking

212 Theoretically, the ranking method can be applied to any event duration. To obtain sensible  
 213 values for the duration of extreme precipitation events in the IWH, we compute the critical  
 214 event duration. We define this value as the duration beyond which the mean ranking magnitude  
 215 of extremes (**R**) remains constant with increasing duration. The mean magnitude of the top 5,  
 216 20, and 100 events increases with event duration and levels off between 5 and 10 days (Fig. 2).  
 217 This agrees with the observation that, for the IWH region, an event lasting longer than 10 days



218 is practically not possible. Thus, we compute 1-day and multi-day rankings up to 10 days. For  
219 brevity, we report the results for 1-, 3-, 5-, 7- and 10-day precipitation rankings.

220 *[Please insert figure here]*

221 **Figure 2: Magnitude ( $R_m$ ) for the first 5, 20 and 100 highest ranked events at various**  
222 **multi-day duration of accumulated precipitation. X-axis denotes duration (i.e. time**  
223 **period) of an event in days. Y-axis denotes the mean magnitude of the event in mm.**

## 224 4 Results and Discussion

225 Section 4.1 reports the seasonal and long-term (113 years) evolution of the magnitude and  
226 frequency of extremes at different duration. Section 4.2 presents the results of the ranking for  
227 IWH and discusses specific events. The ranking of extreme events is based on the magnitude  $R$   
228 that incorporates both percentage area ( $A$ , spatial extension) and mean value (intensity of  
229 extreme precipitation) for different durations. Finally, we shed light on the major limitation of  
230 our approach by discussing specific missed cases in the ranking (Section 4.3).

### 231 4.1 Seasonal and long-term evolution of precipitation extremes

232 Fig. 3 (a&b) shows the decadal progression of frequency and mean magnitude ( $R$ ) of the  
233 extremes in IWH for different durations. There is a sharp increase in both frequency and  
234 magnitude of extreme precipitation in the last three decades. This pattern is in congruence with  
235 EM-DAT data (Figure 1b) confirming an increase in disasters in the Indian Western Himalayan  
236 and also validating our findings. There is also a pronounced seasonal pattern, similar for all  
237 durations, in the occurrence (Fig. 3c) and magnitude (Fig. 3d) of the top 1% events. In both  
238 cases, the maxima occurs around August/September and a less pronounced secondary  
239 maximum is visible in February. This pattern is explained by the two major atmospheric  
240 patterns that are responsible for precipitation over IWH, i.e. ISM from June to September, and  
241 WD dominating from December to March. Interestingly, the frequency of extremes increases  
242 strongly with duration during ISM (Fig. 3c). These results highlight that, similar to other parts  
243 of the world (Marelle *et al.*, 2018), precipitation extremes in IWH have a clear seasonal pattern,  
244 which might be changed due to climate warming. Although outside the scope of this study, an  
245 assessment of seasonal changes in the occurrence of extremes in IWH is worth considering in  
246 future studies.

247

248

249 *[Please insert figure here]*

250 **Figure 3: Distribution of precipitation extremes over IWH. Decadal distribution of (a)**  
251 **frequency, and (b) mean magnitude of top 1% extreme events for different durations.**  
252 **Monthly distribution of (c) frequency (d) and magnitude of top 1% extreme events for**  
253 **different durations.**

#### 254 4.2 Ranking of extreme events

255 In this section, we present results for 1-day, 3-days, 5-days, 7-days and 10-days extreme  
256 precipitation events ranking in the IWH. Results obtained for the top 10 events are shown in SI  
257 Table 1 and Fig. 4. Interestingly, many events are not independent and they overlap at different  
258 durations, as we can observe there are only 15 (out of 50) unique events. Furthermore, it is  
259 clear from Fig. 4 that the different top 10 ranks are dominated by four events that occurred  
260 respectively in September 1995 (green bars), March 1990 (red bars), September 1988 (white  
261 bars), July 1995 (light blue bars).

262

263

264 *[Please insert figure here]*

265 **Figure 4: Magnitude ( $R_m$ ) and rank for the top 10 events at different durations (1, 3, 5, 7,**  
266 **and 10 days) of accumulated precipitation. Arrowhead indicates the direction of**  
267 **increasing values.**

268

269 In particular, the September 1995 and March 1990 events dominate the top 10 ranks with 15  
270 and 13 top ranks, respectively. This dominance exerted by just a few extreme precipitation  
271 episodes is expected to occur at longer durations, since we analyse successive accumulated  
272 precipitation days over relatively long periods. Therefore, 2 or 3 intense precipitation  
273 anomalous days will be sufficient to influence successive periods. In the next subsection, we  
274 present specific cases demonstrating the potential of a single day and multi-day duration  
275 extreme event ranking over IWH.

#### 276 4.2.1 Single-day extreme ranking

277 The 1-day first rank event on 02-08-1997 (Fig. 5a) was widespread, with 49% of IWH showing  
278 precipitation anomalies larger than 2 SD. It reached a magnitude of  $\sim 10$  SD (Fig. 5b). The event  
279 hit the north-eastern section of IWH, with maximum precipitation of 235mm and with  
280 precipitation above 200mm observed at several grid points.

281

282

[Please insert figure here]

283

284

285

286

287

288

289

290

291

292

293

294

295

296

297

298

299

300

301

302

303

304

305

306

307

308

309

310

311

312

313

314

**Figure 5: (a) Spatial distribution of accumulated precipitation (mm) and corresponding standard deviation anomalies (black contour) of a 1-day precipitation event occurring on 02-08-1997. (b) Spatial coverage and magnitude of the extreme event occurring between 31-07-1997 and 05-08-1997. Area means percentage of IWH with precipitation anomalies above 2 SD, magnitude is the mean of anomalies above 2 SD.**

The same event is also present in the 3-days ranking (rank 2 & 10) underlining that it was dominant at the daily scale, but precipitation on the day before and the day after were also relevant (Fig. 5b). In this regard, any ranking methodology focussing on single-day duration (often used in the literature) would be limited in capturing its evolution. The absence of this event from further multi-days ranking (5-, 7-, and 10-days ranking) shows that the extreme event occurred only for 3-4 continuous days (i.e. 1-4 August). This event occurred prior to a highly localised cloud bursting event over Chiragaon village in Shimla district of Himachal Pradesh between 8-14 August 1997 resulting in 135 fatalities along with 20 injuries (Source EM-DAT data; Yogendra, 1999; Pathania, 1997). Interestingly, the precipitation between 8-14 August 1997 was not extreme and hence did not show up in the top 10 ranking. Thus, it is likely that the extreme precipitation on 1-4 August increased the river flow and decreased the capacity of the soil to absorb further rainfall in the following days. This might have strongly increased the vulnerability to landslides during the subsequent cloud bursting event.

The rank 2 event (Fig. S1) of 1-day ranking on 05-09-1995 covered a wider area when compared to the top event, affecting an area of 66% of IWH (>2SD), but with a lower overall intensity with a mean anomaly value  $\sim 6$  SD. The precipitation over some localised grid cells surpassed 300mm, with a maximum value of 425mm (Fig. S1). Most of IWH received rainfall above 150mm. This event is also present at 3-, 5-, 7- and 10-days ranking. This clearly indicates that it is a continuous extreme event expanding over multi-days (at least up to 10 days) and affecting major easterly portions of JK, HP and northwestern portions of UK. The rank 3 event (Fig. S2) of 1-day ranking took place on 09-02-2010 affecting 85% of IWH area (> 2 SD), albeit with comparatively lower intensity  $\sim 5$  SD. This event is absent at 3-, 5-, 7-, and 10-days rankings revealing that it was a single day extreme event. The precipitation on this day attained a maximum value of 127mm. Nevertheless, this event was clearly linked with a landslide causing 17 deaths in Hatia Bala town of JK (Source EM-DAT data; Konagai and Sattar, 2012).

315 Based on these results, we can re-iterate that the ranking method is highly dependent on  
316 combined indices values that take into account simultaneously the magnitude of the event as  
317 well as the total area affected. This method is certainly more effective than a single metric of  
318 spatial spread or intensity at a single day duration.

#### 319 **4.2.2 Multi-day extreme ranking**

320 Several events, which are not significant on a daily ranking, become significant, based on  
321 intensity and spatial extension at longer time durations. For instance, four events appear in the  
322 3-day ranking category (rank 3, 6, 7 & 9) that are absent in the 1-day ranking. The changes in  
323 the ranking of different duration highlight the importance of multi-day ranking of extremes, as  
324 it is crucial to capture events of varying spatiotemporal characteristics. The extreme event of  
325 05-09-1995 accounts for 15 occurrences (green bars in Figure 4). Below, we provide a more  
326 detailed description of the spatio-temporal progression of the event at short (3-day) and long  
327 (10-day) duration.

#### 328 **Event of 05-09-1995 in short and long duration**

329 Figure 6 (Panel I) shows the cumulative rainfall for the short duration time scales of this event,  
330 for which it is ranked first. The short duration event affected an area of 69% of IWH (>2SD)  
331 with a mean anomaly value of ~12.4 SD.

332

333

*[Please insert figure here]*

334 **Figure 6: Panel I- Spatial distribution of accumulated precipitation (mm) and**  
335 **corresponding standard deviation anomalies (black contour) of the 3-days precipitation**  
336 **event on 05-09-1995 i.e. from 03-09-1995 to 05-09-1995. Panel II (a-j)- Spatial**  
337 **distribution of daily precipitation (mm) and corresponding standard deviation**  
338 **anomalies (black contour) of the 10-days period spanning between 28-08-1995 and 06-**  
339 **09-1995. (k) Spatial coverage and magnitude of the extreme event.**

340

341 The event was not a short-lived one and lasted for a considerable longer duration of 10-days  
342 from 28 Aug – 6 Sept 1995 (Fig. 6 (Panel II)). Daily precipitation anomalies higher than 2 SD are  
343 present on all the days except 28-08-1995 (Fig. 6k (Panel II)). Precipitation was localised and  
344 less intense in the first four days (Fig. 6 part II (a-d)). Afterwards it intensified and became  
345 widespread, attaining its peak on 5 September. As reported by Vellore et al. (2016), two storms  
346 hit IWH during these 10 days. The first storm was active on the first four days, while the second

347 storm struck during the last six days (Vellore et al., 2016), as can be concluded from Fig. 6 (Panel  
348 II).

349

350 ● For the first four days, the highest values of precipitation can be observed over an NW-  
351 SE band of IWH affecting mainly HP and the UK. Precipitation during these four days  
352 was relatively scattered and less intense (Fig.6 Panel II (a-d)).

353 ● On the first day, i.e., 28-08-1995, no area got affected above anomaly of 2 SD, and max  
354 precipitation was only up to 41mm. Whereas, on the second and third day affected 2%  
355 and 6% of the IWH area above anomaly of 2 SD and M value on these two days were  
356 equal to 2.9 SD with max precipitation of 67mm and 79mm. Anomalies up to 4 SD were  
357 seen on these two days in regions of the UK.

358 ● On the fourth day, i.e. 31-08-1995 (Fig. 6, Panel II d), this particular pattern of  
359 precipitation receded affecting 2% of area above anomaly benchmark and with a mean  
360 intensity of 3 SD, with precipitation being mainly localised over the lower southernmost  
361 part of the UK with anomalies value over grids up to 4 SD and max precipitation up to  
362 87mm.

363 ● Onward, the fifth day we see precipitation in an entirely NE-SW orientation, i.e. almost  
364 orthogonal to the previous one, affecting mainly the eastern portion of JK. This storm  
365 affected on its first day (1 September) an area of 13% of IWH (>2 SD) with mean anomaly  
366 value of 3 SD and reaching 4 SD locally. This NE-SW precipitation band increased in both  
367 magnitude and area affected until 5 September (Fig. 6, Panel II i).

368 This prolonged event was related to the disastrous floods that took place in HP, JK and almost  
369 the entire northern India (Haryana, Delhi, Punjab, Bihar, Uttar Pradesh) between Sept 1 – Sept  
370 20 causing the death of 1479 people and affecting 32.704.000 people in total  
371 (<https://public.emdat.be/data>;Blaskovic, 2018; Sen, 1995).

372

### 373 **4.3 Strengths and limitations of the ranking approach**

374 To demonstrate the strengths and limitations of our approach, we present two particular events  
375 that are only included at multi-day ranking. Additionally, we discuss why this approach fails to  
376 assign a top rank to the event on 17 June 2013 that triggered the deadliest disaster in  
377 Uttarakhand.

378

#### 379 **4.3.1 Strengths: Capturing disastrous events at multi-day time scales**

### 380 **Case I: 12th July 1993 event**

381 The extreme event on 12-07-1993 (orange bar in Fig. 4) had tremendous socioeconomic  
382 impacts as it heavily flooded the HP and JK states as well as other northwestern states (Punjab,  
383 Haryana, Gujarat, Rajasthan, Chandigarh) of India causing a death toll of 827 and affecting 128  
384 million people (Source: EM-DAT data). The event appears only in the 5-days ranking at the 6th  
385 rank, with indices A and M as 82% and 10.5 SD, respectively. Not all five accumulating days of  
386 this event were severe enough to be included in top 10 of the daily ranking (Fig. 7a). An  
387 assessment of the atmospheric circulation at the synoptic scale by Kulkarni et al. (1995)  
388 showed the combined effect of meteorological configurations responsible for the event. It was  
389 caused mainly due to (i) a well-marked low-pressure system over the region, (ii) a cyclonic  
390 circulation that extended up to mid-tropospheric levels and prevailed over the regions between  
391 9 and 10 July, (iii) an off-shore trough running from the north Maharashtra coast to the Kerala  
392 coast, persisting during the four days between 9-12 July, and (iv) a western disturbance that  
393 lay over north Pakistan and its neighbourhood on 9 July, and moved away from north-eastward  
394 across Jammu and Kashmir on 14 July (Kulkarni et al., 1995).

395

396

*[Please insert figure here]*

397 **Figure 7: Daily evolution of the spatial coverage and magnitude of the extreme events on**  
398 **12-07-1993 (a) and 22-03-1990 (b).**

399

### 400 **Case II: 22nd March 1990 event**

401 The event on 22-03-1990 is linked with massive flooding of JK (Kaluchak, Kargil) over the two  
402 days 21-22 March 1990, causing 69 fatalities. This event is at rank 7 in 3-days ranking (red bar  
403 in Fig. 4) but not in the top 10 of the daily ranking (Table 1). However, unlike the previous case  
404 (which was captured only once at 5-day duration), this event is among the top 10 ranks for all  
405 other durations and occupies 13 out of 50 ranks (Table 1). This is an interesting finding for an  
406 event that remains unnoticed at 1-day scale. Its precipitation is relatively less intense and  
407 localised on the first three days compared to other days where it intensified and became more  
408 widespread (Fig. 7b).

409

410 **4.3.2. Limitation: Why is the deadliest 17th June 2013 Uttarakhand disaster not present**  
411 **in the top 10 extreme events?**

412 In June 2013, Uttarakhand state experienced an extreme 4-day rainfall event leading to  
413 devastating floods and landslides. During the event, 370 mm/day of rain was recorded at  
414 Dehradun corresponding to 27% of the annual rainfall (Gosain et al., 2015). Heavy rainfall caused  
415 a breach in a moraine dammed lake, leading to severe flooding that resulted in the loss of  
416 thousands of lives, and massive infrastructure damage that affected 4200 villages, 1636 roads,  
417 144 bridges, and 19 hydropower plants (Das, 2013, Rautela, 2013, Dube et al., 2014, Kala, 2014,  
418 Gosain et al., 2016). This event is considered as India's worst natural disaster since the December  
419 2004 Indian Ocean tsunami (Dubey et al., 2013; Kumari *et al.*, 2019). Reconstruction cost after the  
420 disaster is estimated to be almost 480 million pounds (Jogesh et al 2016; Kumari *et al.*, 2019). We  
421 analysed the data from 14 to 17th June 2013 to understand why the deadliest disaster in  
422 Uttarakhand is missing from the top 10 ranks for the 1-day and multi-day extremes. 17th June  
423 was the most extreme day of this event (mean magnitude  $M = 225$  mm; rank 38), followed by 16  
424 June ( $M = 156$  mm; rank 96). We compared these events with the 1-day top 1 event of 02-08-1997  
425 and the top 3 event of 09-02-2010 (Table 2, Fig. 8). Although day 17-06-2013 holds a mean  
426 magnitude of 8.3 SD, it is a localised event affecting only 27% of the IWH area. Day 16-06-2013 is  
427 more widespread, affecting 40%, but considerably less intense with a mean magnitude of 3.4 SD.  
428 In comparison, the rank 1 event on 02-08-1997 (Fig. 8d) affected almost half the area of IWH  
429 with a high intensity ( $M = 9.9$  SD). Likewise, the rank 3 event on 09-02-2010 (fig. 8c) had an even  
430 larger spatial spread ( $A = 85\%$ ), albeit a lower intensity of 4.4 SD. Besides, the intensity of  
431 Uttarakhand disaster accumulating days was localised with some specific regions receiving  
432 extremely high rainfall in comparison to others. Hence, the mean value of intensity did not reach  
433 high value because of the small spatial extent of the event. The high intensity, but low affected  
434 area represent important characteristics of this event and are compatible with the disaster-  
435 affected communities, as most of them were concentrated in the Mandakini catchment  
436 (Kedarnath valley in Uttarakhand state of IWH) and surrounding regions (India Disaster Report  
437 2013). Our results agree with Mishra and Srinivasan (2013) who highlighted that rainfall during  
438 the Uttarakhand floods was not the most intense rainfall this region has ever faced, however, it  
439 was considered one of India's worst disasters due to the subsequent impact on society.

440 We would also like to reiterate that not all extreme precipitation events are associated with  
441 geomorphological disasters with significant human and socioeconomic impacts. Some disasters,  
442 such as the Uttarakhand 2013 event, result from a number of contributing factors and the relation  
443 between precipitation and impact is typically nonlinear (e.g. Kreibich *et al.*, 2017). Natural  
444 hazards are transformed into disasters due to socioeconomic factors, such as rising population,  
445 poorly regulated tourism industry, and poor infrastructure development including road network

446 expansion in environmentally sensitive zones (Ziegler et al., 2014; Bhambri et al., 2016). Extreme  
447 events have occurred in Uttarakhand previously (Dimri, 2013). But the large number of human  
448 casualties and the massive damage observed in the June 2013 extreme event can be broadly  
449 attributed to two additional reasons: (1) coincidence of the annual pilgrimage with the event  
450 exposing a large number of people to the hazard, and (2) heavy rainfall on the preceding days of  
451 June 10 and 11, 2013 that saturated the soil and made the ground vulnerable to landsliding.  
452 Furthermore various other anthropogenic factors, such as unchecked and rapid land-use changes  
453 and urban infrastructure development, enhanced the intensity and scale of the impact (Kala,  
454 2014). Finally, the Indian monsoon system reached the region two weeks earlier than normal in  
455 June 2013 (Joseph et al., 2015) and hence, the region was not prepared for that. Therefore, the  
456 compounding effect of various factors in combination with the relatively high precipitation values  
457 caused disastrous impacts (Sharma et al., 2013).

458

459

*[Please insert figure here]*

460 **Figure 8: Spatial distribution of accumulated precipitation (mm) and corresponding**  
461 **standard deviation anomalies (black contour) during the Uttarakhand 2013 disaster and**  
462 **the top-ranked event at 1-day. (a-b) represent days during Uttarakhand floods, (c) and**  
463 **(d) are the rank 3 and rank 1 event, respectively.**

464

465 Overall our results highlight that the developed ranking scheme is not biased to extreme events  
466 that affect small areas only even when these t can impinge catastrophic impacts at a more local  
467 scale. The method was developed to consider both the level of spatial-spread (metric A), as well  
468 as the intensity of the event (metric M) in the affected area. Both metrics are essential to calculate  
469 a representative ranking magnitude, which is the basis of comparison of different precipitation  
470 events. The case studies in sections 4.3.1 and 4.3.2 highlight that there is a further need to reduce  
471 the spatial scale of a domain to state or even basin to obtain a more extensive analysis of extreme  
472 precipitation events for that smaller spatial scale, but that are relevant to shape effective disaster  
473 and hydrological policies there.

## 474 5 Conclusions

475 We ranked extreme precipitation events in Indian Western Himalayan (IWH) accounting for  
476 precipitation magnitude and spatial extent at different duration. Events are ranked higher due  
477 to particularly high precipitation magnitudes, whereas other events are characterized by



478 extensive spatial spread or due to persistent rainy conditions for a longer duration. We observe  
479 that the ranking method apart from identifying such long-duration extremes are also useful in  
480 determining the timing of the maximum impact. Our analysis reveals the benefits of using a  
481 multi-day ranking scheme to better quantify and track the spatial and temporal propagation of  
482 the extreme. The different rankings databases obtained considering the various durations are  
483 useful for other studies focused on the impacts of extreme precipitation periods covering  
484 relatively large areas, but also useful for studies assessing the evolution of the atmospheric  
485 circulation during those days.

486 Future studies can link the analysis of extremes with associated socio-economic impacts. One  
487 way to do this is to add a fourth metric of population exposed to the extremes, thereby giving a  
488 higher rank to the events that occur in densely populated areas. As per the results of present  
489 study, it is true that there is not any direct relation between the positions of events in the table  
490 and the socioeconomic impacts as there are a number of other factors responsible. But our  
491 approach indeed determines that if we keep all other varying factors constant then the  
492 probability of the socioeconomic effects are well correlated with the ranking position. Our  
493 classification scheme is also useful, as shown in several case studies, to determine which time  
494 scale is more likely to bring socioeconomic impacts. In many cases, socioeconomic impacts are  
495 not just a result of short and intense events but also accumulated moderate events for a more  
496 extended period, which then become significant.

#### 497 **Acknowledgement**

498 SR and AA acknowledge the generous funding support by SPARK summer internship program  
499 at IIT Roorkee. The work was further supported under the COPREPARE project  
500 (<https://ir.iitr.ac.in/COPREPARE/>) funded by University Grant Commission (UGC) and DAAD.

#### 501 **Competing interest**

502 The authors declare no conflict of interest.

#### 503 **References**

- 504 Beguería, S., Vicente-Serrano, S.M., López-Moreno, J.I., García-Ruiz, J.M., 2009. Annual and seasonal mapping of  
505 peak intensity, magnitude and duration of extreme precipitation events across a climatic gradient,  
506 northeast Spain. *Int. J. Climatol.* 29, 1759–1779. <https://doi.org/10.1002/joc.1808>
- 507 Blaskovic, T., 2018. Worst floods since 1995 hit Himachal Pradesh, India.
- 508 Das, L., Meher, J.K., 2019. Drivers of climate over the Western Himalayan region of India: A review. *Earth-Sci. Rev.*  
509 198, 102935. <https://doi.org/10.1016/j.earscirev.2019.102935>

- 510 D.Guha-Sapir, D. EM-DAT: The Emergency Events Database. Available online: [www.emdat.be](http://www.emdat.be) (accessed on 20  
511 August 2020)
- 512 Dung, N. V., Merz, B., Bárdossy, A., & Apel, H. (2015). Handling uncertainty in bivariate quantile estimation - An  
513 application to flood hazard analysis in the Mekong Delta. *Journal of Hydrology*, 527, 704-717.  
514 doi:10.1016/j.jhydrol.2015.05.033
- 515 Ghosh, S., Das, D., Kao, S.-C., Ganguly, A.R., 2012. Lack of uniform trends but increasing spatial variability in  
516 observed Indian rainfall extremes. *Nat. Clim. Change* 2, 86-91. <https://doi.org/10.1038/nclimate1327>
- 517 Guntu, R.K., Maheswaran, R., Agarwal, A., Singh, V.P., 2020. Accounting for temporal variability for improved  
518 precipitation regionalization based on self-organizing map coupled with information theory. *J. Hydrol.*  
519 590, 125236. <https://doi.org/10.1016/j.jhydrol.2020.125236>
- 520 Kahlon et al, 2014. Landslides in Himalyan Mountains: A study of Himachal Pradesh, India. *International Journal*  
521 *of IT, Engineering and Applied Sciences Research (IJIEASR) I 3*, 28-34.
- 522 Konagai, K., Sattar, A., 2012. Partial breaching of Hattian Bala Landslide Dam formed in the 8th October 2005  
523 Kashmir Earthquake, Pakistan. *Landslides* 9, 1-11. <https://doi.org/10.1007/s10346-011-0280-x>
- 524 Krishnamurti, T.N., Martin, A., Krishnamurti, R., Simon, A., Thomas, A., Kumar, V., 2013. Impacts of enhanced CCN  
525 on the organization of convection and recent reduced counts of monsoon depressions. *Clim. Dyn.* 41,  
526 117-134. <https://doi.org/10.1007/s00382-012-1638-z>
- 527 Krishnan, R., Shrestha, Arun B., Ren, G., Rajbhandari, R., Saeed, S., Sanjay, J., Syed, Md.A., Vellore, R., Xu, Y., You, Q.,  
528 Ren, Y., 2019. Unravelling Climate Change in the Hindu Kush Himalaya: Rapid Warming in the Mountains  
529 and Increasing Extremes, in: Wester, P., Mishra, A., Mukherji, A., Shrestha, Arun Bhakta (Eds.), *The Hindu*  
530 *Kush Himalaya Assessment*. Springer International Publishing, Cham, pp. 57-97.  
531 [https://doi.org/10.1007/978-3-319-92288-1\\_3](https://doi.org/10.1007/978-3-319-92288-1_3)
- 532 Kulkarni et al, 1995. ANALYSIS OF SEVERE RAINSTORMS OVER GUJARAT AND PUNJAB DURING THE 1993  
533 MONSOON.
- 534 Kumari, S., Haustein, K., Javid, H., Burton, C., Allen, M.R., Paltan, H., Dadson, S., Otto, F.E.L., 2019. Return period of  
535 extreme rainfall substantially decreases under 1.5 °C and 2.0 °C warming: a case study for Uttarakhand,  
536 India. *Environ. Res. Lett.* 14, 044033. <https://doi.org/10.1088/1748-9326/ab0bce>
- 537 Kreibich, H., Di Baldassarre, G., Vorogushyn, S., Aerts, J. C. J. H., Apel, H., Aronica, G. T., ... Merz, B. (2017). Adaptation  
538 to flood risk: Results of international paired flood event studies. *Earth's Future*, 5(10), 953-965.  
539 doi:10.1002/2017ef000606
- 540 Krishnan R, Sabin TP, Madhura RK, Vellore RK, Mujumdar M, Sanjay J, Nayak S, Rajeevan M. 2019. Non-monsoonal  
541 precipitation response over the Western Himalayas to climate change. *Climate Dynamics*, 52(7-8): 4091-  
542 4109. <https://doi.org/10.1007/s00382-018-4357-2>.
- 543 Müller, M., Kaspar, M., 2014. Event-adjusted evaluation of weather and climate extremes. *Nat. Hazards Earth*  
544 *Syst. Sci.* 14, 473-483. <https://doi.org/10.5194/nhess-14-473-2014>
- 545 Marelle L, Myhre G, Hodnebrog Ø, Sillmann J, Samset BH. 2018. The Changing Seasonality of Extreme Daily  
546 Precipitation. *Geophysical Research Letters*, 45(20). <https://doi.org/10.1029/2018GL079567>.
- 547 Nandargi, S., Dhar, O.N., 2011. Extreme rainfall events over the Himalayas between 1871 and 2007. *Hydrol. Sci. J.*  
548 56, 930-945. <https://doi.org/10.1080/02626667.2011.595373>
- 549 Nandargi, S., Gaur, A., Mulye, S.S., 2016. Hydrological analysis of extreme rainfall events and severe rainstorms  
550 over Uttarakhand, India. *Hydrol. Sci. J.* 61, 2145-2163.

- 551 <https://doi.org/10.1080/02626667.2015.1085990>
- 552 Natural Disaster Management, n.d.
- 553 N. Nicholls, D. Easterling, C.M. Goodess, S. Kanae, J. Kossin, Y. Luo, J. Marengo, K. McInnes, M. Rahimi, M. Reichstein,  
554 A. Sorteberg, C. Vera, and X. Zhang, 2012: Changes in climate extremes and their impacts on the natural  
555 physical environment. In: *Managing the Risks of Extreme Events and Disasters to Advance Climate Change  
556 Adaptation* [Field, C.B., V. Barros, T.F. Stocker, D. Qin, D.J. Dokken, K.L. Ebi, M.D. Mastrandrea, K.J. Mach, G.-  
557 K. Plattner, S.K. Allen, M. Tignor, and P.M. Midgley (eds.)]. A Special Report of Working Groups I and II of  
558 the Intergovernmental Panel on Climate Change (IPCC). Cambridge University Press, Cambridge, UK, and  
559 New York, NY, USA, pp. 109-230.
- 560 Ozturk, U., Marwan, N., Korup, O., Saito, H., Agarwal, A., Grossman, M.J., Zaiki, M., Kurths, J., 2018. Complex  
561 networks for tracking extreme rainfall during typhoons. *Chaos Interdiscip. J. Nonlinear Sci.* 28, 075301.  
562 <https://doi.org/10.1063/1.5004480>
- 563 Pahauri et al, 2014. *Climate Change 2014: Synthesis Report*.
- 564 Pai, D.S., Sridhar, L., Rajeevan, M., Sreejith, O., Satbhai, N., Mukhopadhyay, N., 2014. Development of a new high  
565 spatial resolution (0.25° × 0.25°) Long Period (1901-2010) daily gridded rainfall data set over India and  
566 its comparison with existing data sets over the region.
- 567 Pandit, M.K., 2013. The Himalayas must be protected. *Nature* 501, 283–283. <https://doi.org/10.1038/501283a>
- 568 Parry et al, 2007. *Climate Change 2007: Impacts, Adaptation and Vulnerability*.
- 569 Pathania, K., 1997. At least 140 killed in floods in northern India.
- 570 Priya, P., Krishnan, R., Mujumdar, M., Houze, R.A., 2017. Changing monsoon and midlatitude circulation  
571 interactions over the Western Himalayas and possible links to occurrences of extreme precipitation.  
572 *Clim. Dyn.* 49, 2351–2364. <https://doi.org/10.1007/s00382-016-3458-z>
- 573 Rajeevan et al, 2006. A High Resolution Daily Gridded Rainfall Data for the Indian Region: Analysis of break and  
574 active monsoon spells. *Curr Sci* 91.
- 575 Ramos, A.M., Trigo, R.M., Liberato, M.L.R., 2017. Ranking of multi-day extreme precipitation events over the  
576 Iberian Peninsula: MULTI-DAY EXTREME PRECIPITATION EVENTS IBERIAN PENINSULA. *Int. J. Climatol.*  
577 37, 607–620. <https://doi.org/10.1002/joc.4726>
- 578 Ramos, A.M., Trigo, R.M., Liberato, M.L.R., 2014. A ranking of high-resolution daily precipitation extreme events  
579 for the Iberian Peninsula: Ranking of the Iberian Peninsula daily precipitation. *Atmospheric Sci. Lett.*  
580 n/a-n/a. <https://doi.org/10.1002/asl2.507>
- 581 Ren, F., Cui, D., Gong, Z., Wang, Y., Zou, X., Li, Y., Wang, S., Wang, X., 2012. An Objective Identification Technique  
582 for Regional Extreme Events. *J. Clim.* 25, 7015–7027. <https://doi.org/10.1175/JCLI-D-11-00489.1>
- 583 Sen, A., 1995. Poor drainage, inept river management, heavy rains lead to one of north India's worst floods.
- 584 Shukla, R., Agarwal, A., Gornott, C., Sachdeva, K., Joshi, P.K., 2019a. Farmer typology to understand differentiated  
585 climate change adaptation in Himalaya. *Sci. Rep.* 9, 20375. <https://doi.org/10.1038/s41598-019-56931-9>
- 586 9
- 587 Shukla, R., Agarwal, A., Sachdeva, K., Kurths, J., Joshi, P.K., 2019b. Climate change perception: an analysis of  
588 climate change and risk perceptions among farmer types of Indian Western Himalayas. *Clim. Change*  
589 152, 103–119. <https://doi.org/10.1007/s10584-018-2314-z>
- 590 Satendra, K. J. Anandha Kumar, V. K. Naik, 2014. *INDIA DISASTER REPORT 2013*. National Institute of Disaster  
591 Management.

- 592 Uhlemann, S., Thielen, A. H., & Merz, B. (2010). A consistent set of trans-basin floods in Germany between 1952–  
593 2002. *Hydrology and Earth System Sciences*, 14(7), 1277-1295. doi:10.5194/hess-14-1277-2010
- 594 Vellore, R.K., Kaplan, M.L., Krishnan, R., Lewis, J.M., Sabade, S., Deshpande, N., Singh, B.B., Madhura, R.K., Rama  
595 Rao, M.V.S., 2016. Monsoon-extratropical circulation interactions in Himalayan extreme rainfall. *Clim.*  
596 *Dyn.* 46, 3517–3546. <https://doi.org/10.1007/s00382-015-2784-x>
- 597 Yogendra, K., 1999. Can flash floods be prevented in HP?
- 598 Zolina, O., Simmer, C., Belyaev, K., Gulev, S.K., Koltermann, P., 2013. Changes in the Duration of European Wet and  
599 Dry Spells during the Last 60 Years. *J. Clim.* 26, 2022–2047. <https://doi.org/10.1175/JCLI-D-11-00498.1>

600  
601  
602  
603  
604  
605  
606  
607  
608

## 609 **Supplementary Information**

610

### 611 **Fig. S1**

612

*[Please insert figure here]*

613 **Figure S1: Spatial distribution and precipitation intensity of a particular event occurred**  
614 **on 05-09-1995.**

615

*[Please insert figure here]*

616 **Figure S2: Spatial distribution and precipitation intensity of a particular precipitation**  
617 **event occurred on 09-02-2010.**

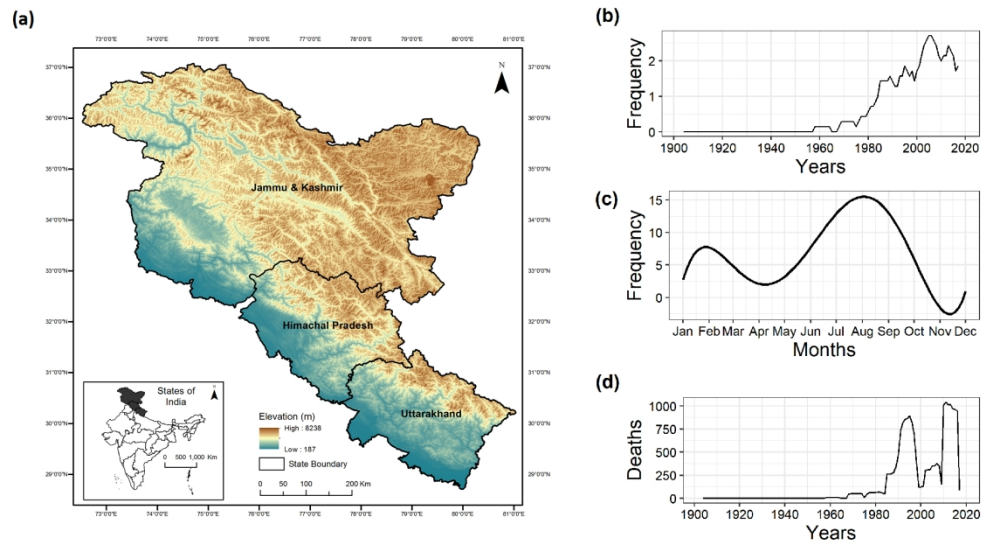


Figure 1: (a) Topography of the Indian Western Himalayas (IWH) consisting of the three states Jammu & Kashmir (JK), Himachal Pradesh (HP) and Uttarakhand (UK), (b) annual frequency and (c) seasonal frequency of occurrence of precipitation-related disasters in the IWH region since 1900 as per EM-DAT data (D. Guha-Sapir et al n.d.,) (d) annual number of deaths in the IWH region due to hydro-climatological hazards as per EM-DAT data.

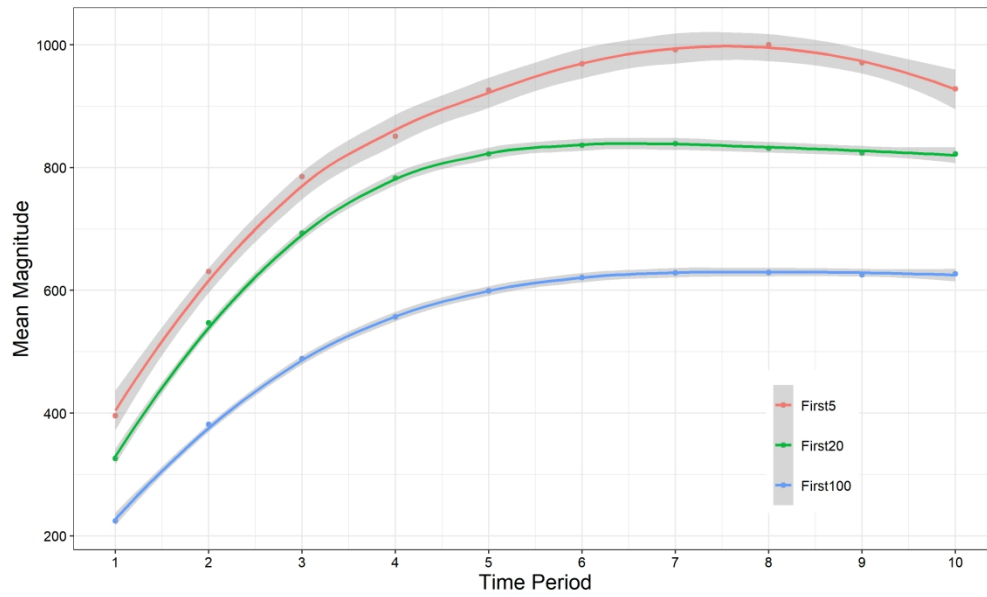


Figure 2: Magnitude ( $R_m$ ) for the first 5, 20 and 100 highest ranked events at various multi-day duration of accumulated precipitation. X-axis denotes duration (i.e. time period) of an event in days. Y-axis denotes the mean magnitude of the event in mm.

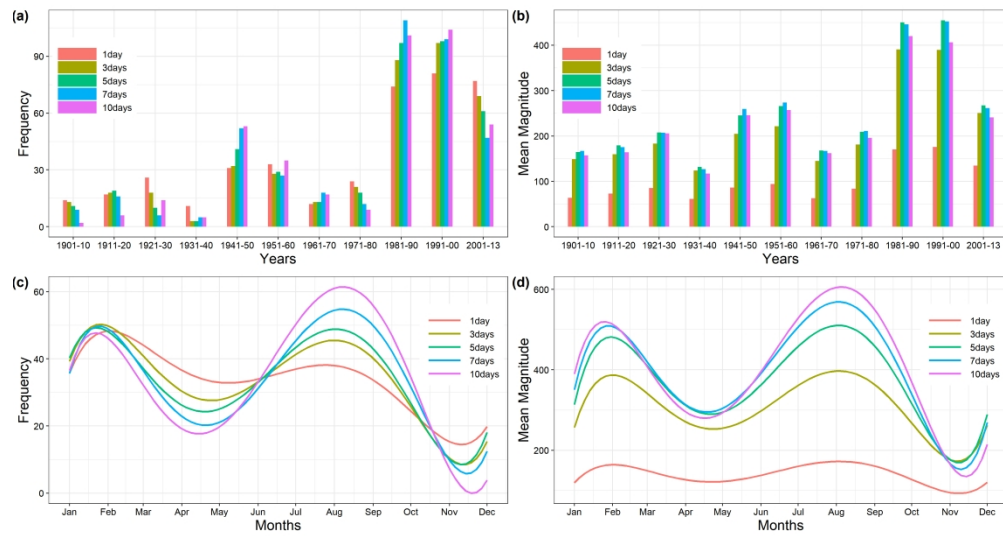


Figure 3: Distribution of precipitation extremes over IWH. Decadal distribution of (a) frequency, and (b) mean magnitude of top 1% extreme events for different durations. Monthly distribution of (c) frequency (d) and magnitude of top 1% extreme events for different durations.

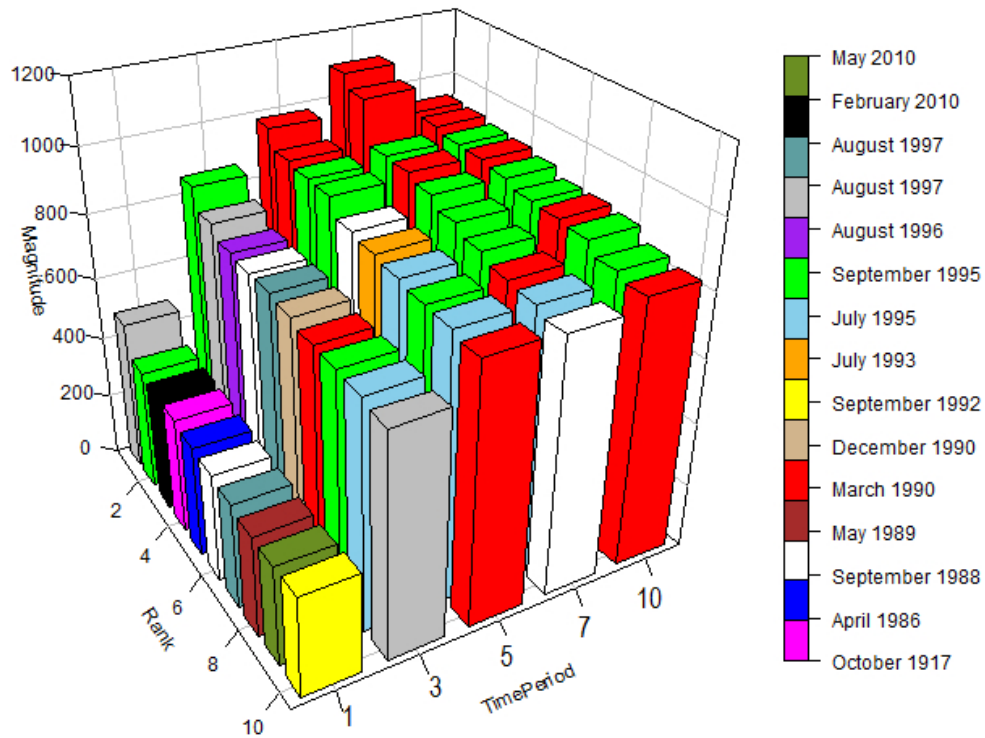


Figure 4: Magnitude ( $R_m$ ) and rank for the top 10 events at different durations (1, 3, 5, 7, and 10 days) of accumulated precipitation. Arrowhead indicates the direction of increasing values.



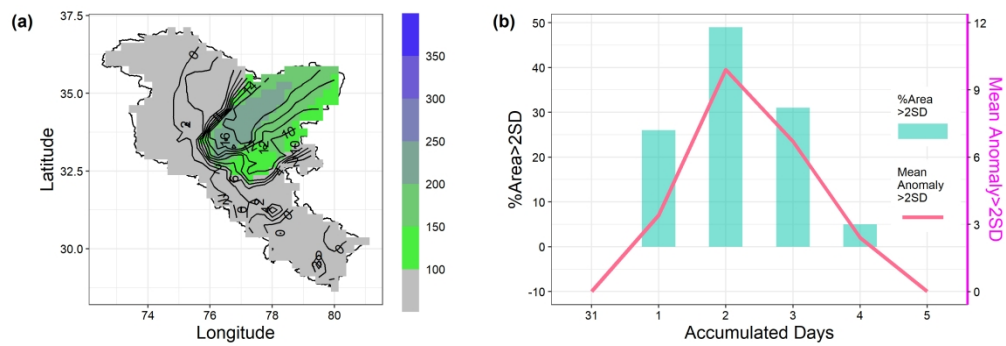


Figure 5: (a) Spatial distribution of accumulated precipitation (mm) and corresponding standard deviation anomalies (black contour) of a 1-day precipitation event occurring on 02-08-1997. (b) Spatial coverage and magnitude of the extreme event occurring between 31-07-1997 and 05-08-1997. Area means percentage of IWH with precipitation anomalies above 2 SD, magnitude is the mean of anomalies above 2 SD.

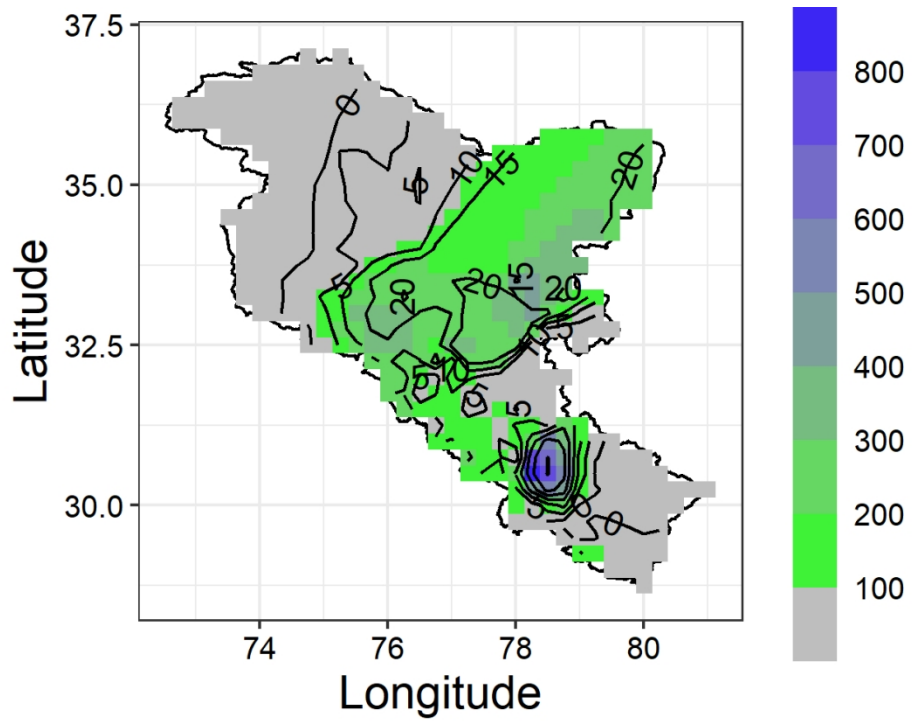


Fig. 6 Panel I- Spatial distribution of accumulated precipitation (mm) and corresponding standard deviation anomalies (black contour) of the 3-days precipitation event on 05-09-1995 i.e. from 03-09-1995 to 05-09-1995.

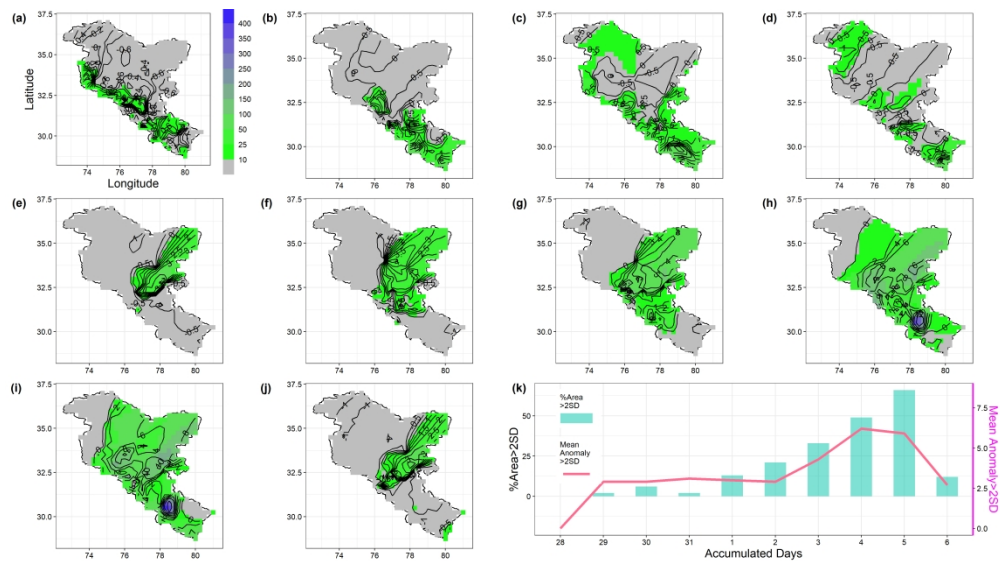


Figure 6: Panel II (a-j)- Spatial distribution of daily precipitation (mm) and corresponding standard deviation anomalies (black contour) of the 10-days period spanning between 28-08-1995 and 06-09-1995. (k) Spatial coverage and magnitude of the extreme event.

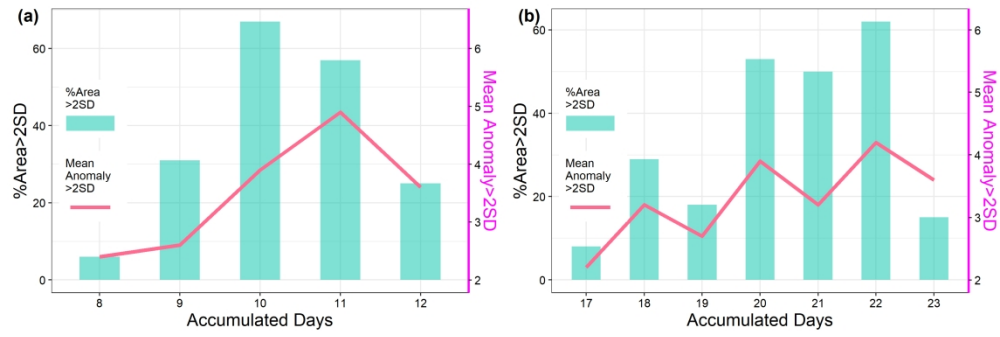


Figure 7: Daily evolution of the spatial coverage and magnitude of the extreme events on 12-07-1993 (a) and 22-03-1990 (b).

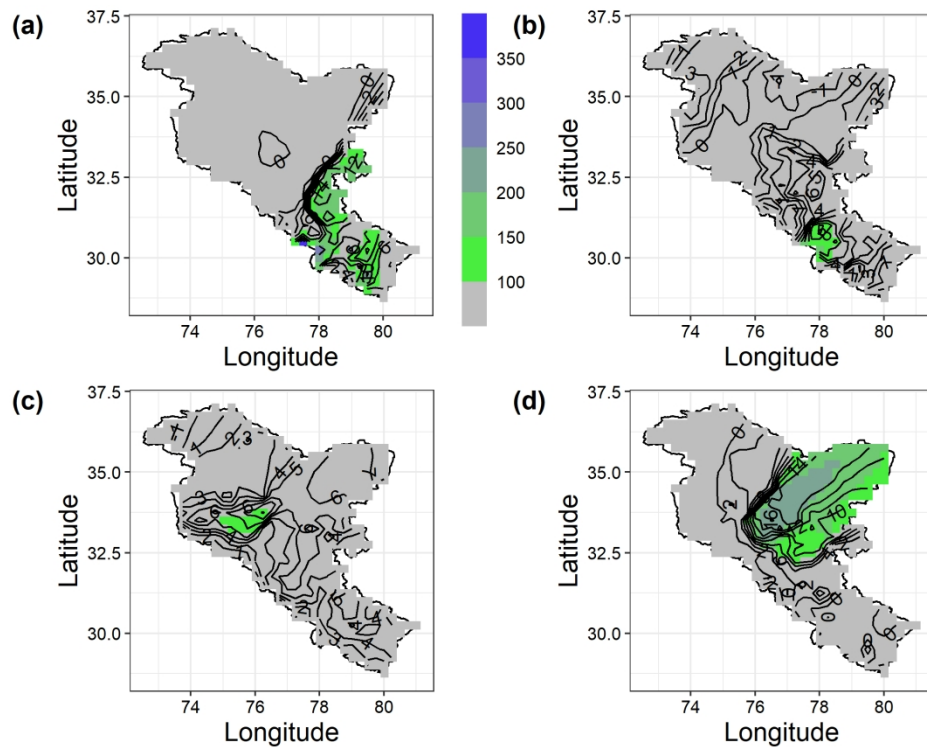


Figure 8: Spatial distribution of accumulated precipitation (mm) and corresponding standard deviation anomalies (black contour) during the Uttarakhand 2013 disaster and the top-ranked event at 1-day. (a-b) represent days during Uttarakhand floods, (c) and (d) are the rank 3 and rank 1 event, respectively.

**Table 1: Top 10 extreme precipitation events in the Indian Western Himalayan for different durations (1, 3, 5, 7 and 10 days). For multi-day durations, dates correspond to the preceding days of accumulated precipitation. Thus, the 3-day top event on the 05-09-1995 corresponds to precipitation registered on 3, 4 and 5 of September.**

<b>Rank</b>	<b>1-Day</b>	<b>3-day</b>	<b>5-day</b>	<b>7-day</b>	<b>10-day</b>
<b>1</b>	02-08-1997	05-09-1995	22-03-1990	23-03-1990	24-03-1990
<b>2</b>	05-09-1995	03-08-1997	23-03-1990	24-03-1990	25-03-1990
<b>3</b>	09-02-2010	24-08-1996	05-09-1995	05-09-1995	06-09-1995
<b>4</b>	27-10-1917	26-09-1988	06-09-1995	22-03-1990	26-03-1990
<b>5</b>	25-04-1986	29-08-1997	27-09-1988	06-09-1995	07-09-1995
<b>6</b>	25-09-1988	30-12-1990	12-07-1993	07-09-1995	08-09-1995
<b>7</b>	28-08-1997	22-03-1990	29-07-1995	08-09-1995	23-03-1990
<b>8</b>	02-05-1989	06-09-1995	07-09-1995	25-03-1990	05-09-1995
<b>9</b>	29-05-2010	28-07-1995	28-07-1995	29-07-1995	09-09-1995
<b>10</b>	10-09-1992	04-08-1997	24-03-1990	28-09-1988	27-03-1990

**Table 2: Ranking index of contributing days to the disastrous Uttarakhand 2013 disaster as compared to the top-ranked event.**

<b>Plot</b>	<b>Date</b>	<b>% Area</b>	<b>Mean Anomaly</b>	<b>Ranking Index</b>	<b>Rank</b>
(a)	17-06-2013	27	8.3	225	38
(b)	16-06-2013	40	3.9	156	96
(c)	09-02-2010	85	4.4	378	3
(d)	02-08-1997	49	9.9	483	1

## Ranking and Characterization of Precipitation Extremes for the past 113 years for Indian western Himalayas

Saurav Raj<sup>1</sup>, Roopam Shukla<sup>2</sup>, Ricardo M. Trigo<sup>3</sup>, Bruno Merz<sup>4</sup>, Maheswaran Rathinasamy<sup>5</sup>, Alexandre M. Ramos<sup>3</sup>, Ankit Agarwal<sup>4,6,\*</sup>

<sup>1</sup>Department of Civil Engineering, Indian Institute of Technology Roorkee, 247667 Uttarakhand, India

<sup>2</sup>Potsdam Institute for Climate Impact Research (PIK), Member of the Leibniz Association, Telegrafenberg, 14473 Potsdam, Germany

<sup>3</sup>Instituto Dom Luiz, Faculdade de Ciências, Universidade de Lisboa, 1749016 Lisboa, Portugal

<sup>4</sup>GFZ German Research Centre for Geosciences, Section 4.4: Hydrology, Telegrafenberg, Potsdam, 14473 Germany

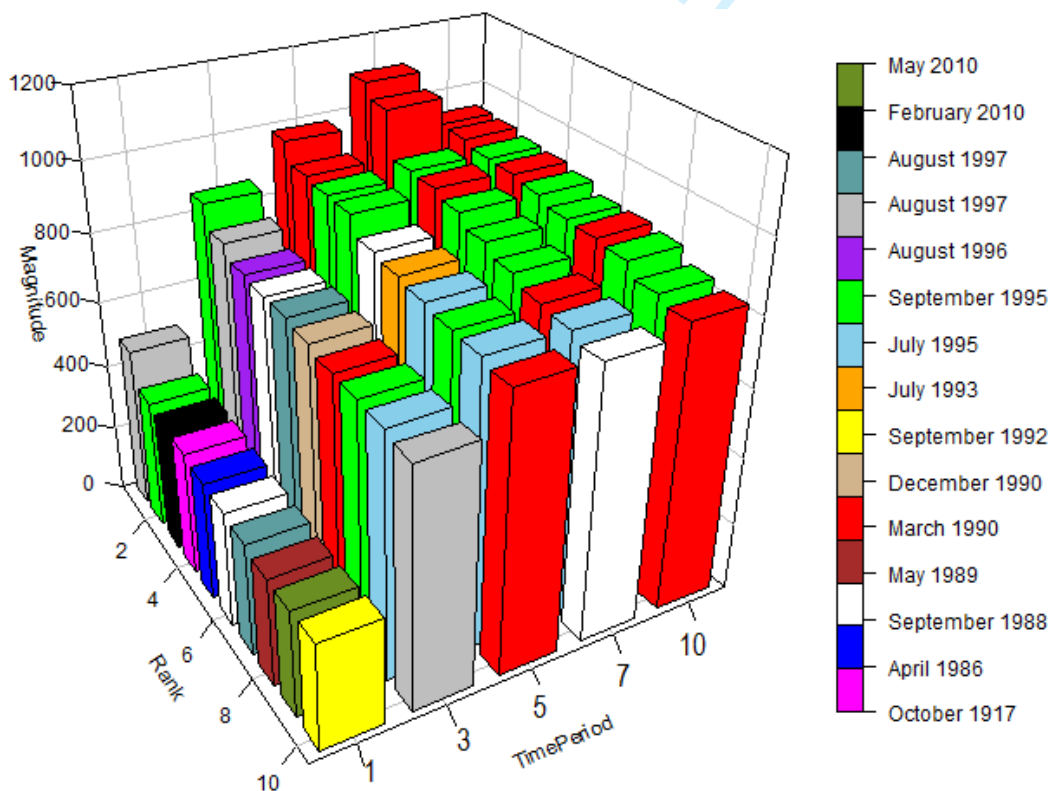
<sup>5</sup>Department of Civil Engineering, MVGR College of Engineering, Vizianagaram, 535005 India

<sup>6</sup>Department of Hydrology, Indian Institute of Technology Roorkee, 247667 Uttarakhand, India

\*Correspondence to: Ankit Agarwal (ankit.agarwal@hy.iitr.ac.in)

### Highlights

- We use 113 years of precipitation data to rank precipitation extreme events in the Indian Western Himalayas, integrating precipitation spatial extent and its intensity across different time-scales
- Results show that the method accurately detects and ranks the most extreme precipitation events that occurred while delineating the spatial contours of these events.
- The proposed ranking method advances conventional single-day event ranking methods by accounting for multi-day duration providing meaningful information on the event duration associated with the highest impact on society.





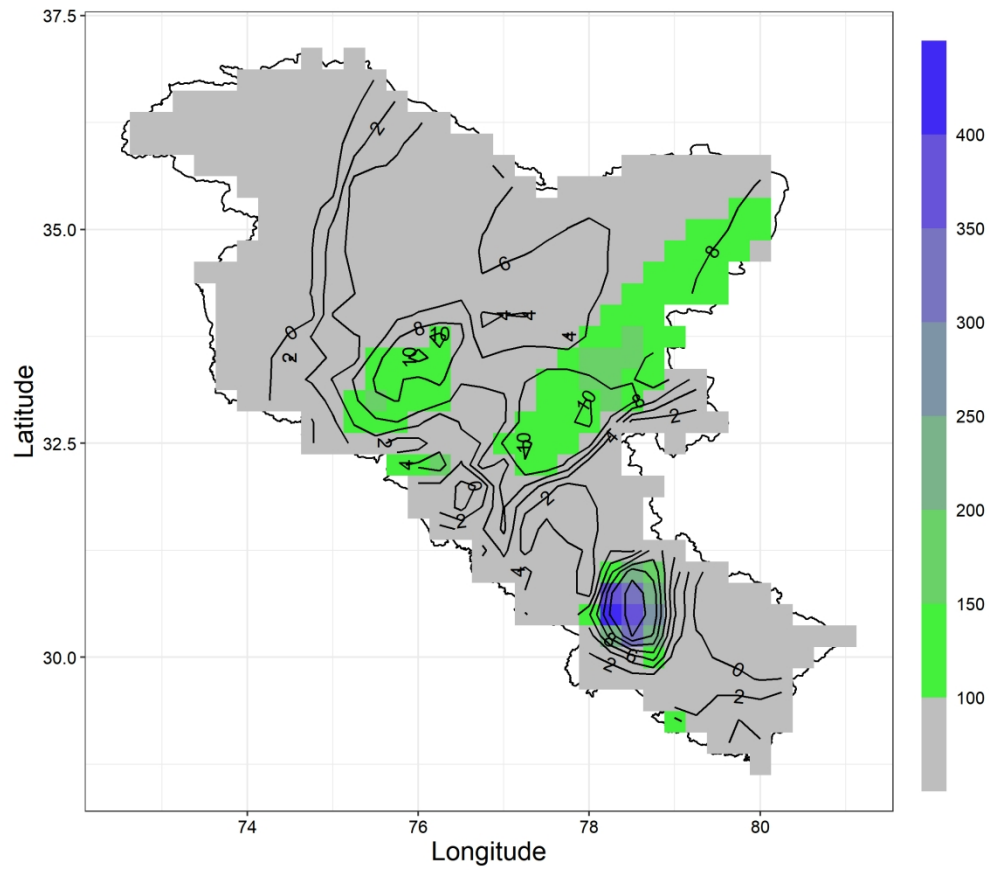


Figure S1: Spatial distribution and precipitation intensity of a particular event occurred on 05-09-1995.

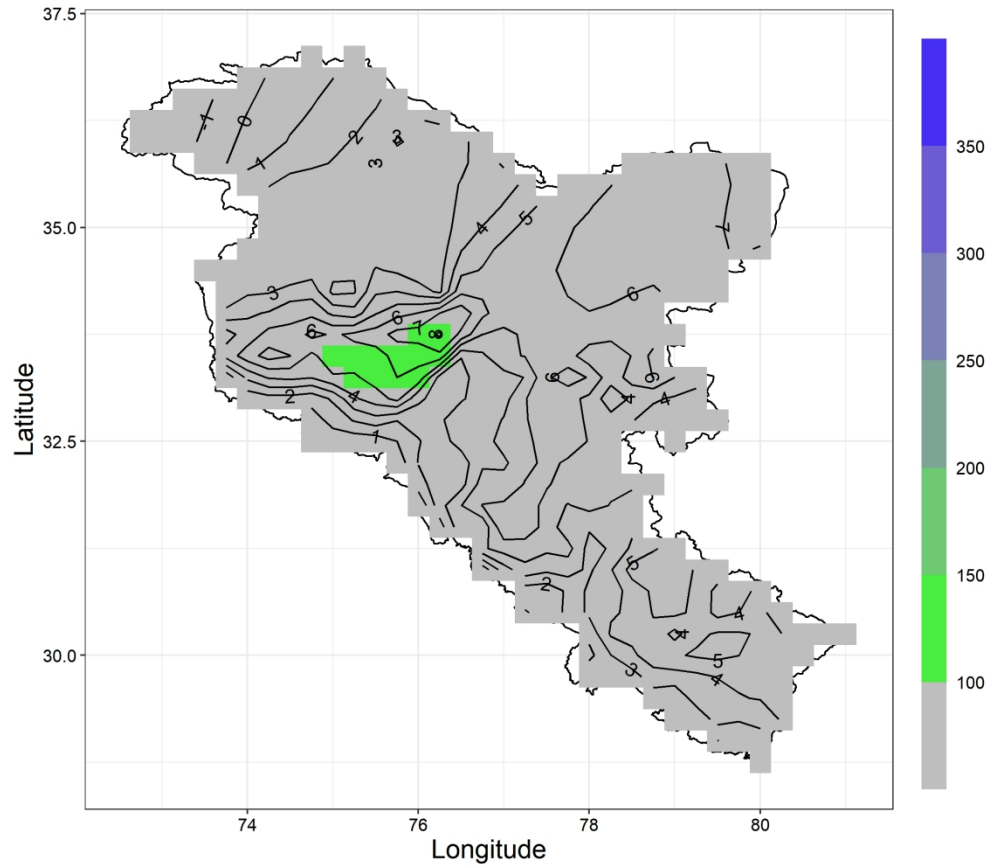


Figure S2: Spatial distribution and precipitation intensity of a particular precipitation event occurred on 09-02-2010.